

## Optical Second Harmonic Spectroscopy of Boron-Reconstructed Si(001)

D. Lim,<sup>1</sup> M. C. Downer,<sup>1\*</sup> J. G. Ekerdt,<sup>1</sup> N. Arzate,<sup>2</sup> Bernardo S. Mendoza,<sup>2</sup> V. I. Gavrilenko,<sup>3</sup> and R. Q. Wu<sup>3</sup>

<sup>1</sup>Texas Materials Institute, University of Texas at Austin, Austin, Texas 78712

<sup>2</sup>Centro de Investigaciones en Optica, A. C. León, Guanajuato, México

<sup>3</sup>Department of Physics and Astronomy, California State University, Northridge, California 91330

(Received 15 December 1999)

Optical second harmonic generation (SHG) spectroscopy is used to probe Si(001) following thermal decomposition of diborane at the surface. Incorporation of boron (B) at second layer substitutional sites at H-free Si(001) intensifies and redshifts the  $E_1$  SHG spectral peak, while subsequent H termination further intensifies and blueshifts  $E_1$ , in sharp contrast to the effect of bulk B doping or nonsubstitutional B. *Ab initio* pseudopotential and semiempirical tight binding calculations independently reproduce these unique trends, and attribute them to the surface electric field associated with charge transfer to electrically active B acceptors, and rehybridization of atomic bonds.

PACS numbers: 73.20.-r, 42.65.Ky, 68.55.Ln, 78.66.-w

Boron (B) is the most widely used bulk dopant in Si-based semiconductor technology. Stable two-dimensional layers of highly B-doped Si with unique structural and electronic properties can be fabricated by depositing B at Si surfaces. Extensive experimental [1–5] and theoretical [6,7] structural studies of such layers have shown that B, unlike larger Group III atoms, enters substitutional sites below the top Si layer, resulting in strong charge transfer from the surface Si to the underlying B acceptors. This charge transfer appears to strongly influence the unique properties of reconstructed B-Si(001) [3,6] and B-Si(111) [1], notably their unusual structures, their reduced chemical reactivity compared to clean surfaces [8–10], and their stability to deposition of Si overlayers, which enables fabrication of ordered-doped structures [4,11].

In this Letter, we report to our knowledge the first surface second harmonic generation (SHG) spectroscopy study of the B-doped Si(001) surface. SHG is sensitive at the monolayer (ML) level to the surface discontinuity of centrosymmetric materials such as Si [12]. Our present results show unique SHG spectroscopic signatures of second layer B incorporation which contrast markedly with those of other Si-adsorbate surfaces [13–16]. Microscopic theory demonstrates a remarkable contribution of vertical surface fields originating from charge transfer to electrically active B in governing SHG spectroscopy. SHG thus complements structure-sensitive probes by directly probing charge transfer which underlies B-Si surface chemistry.

Experiments were performed in an ultrahigh vacuum (UHV) chamber equipped for film growth by chemical vapor deposition (CVD) and multitechnique surface analysis, as described elsewhere [14]. Native oxide was removed by heating the Si(001) sample to 1000 °C. A 0.4  $\mu\text{m}$  thick Si epilayer was then grown by CVD from disilane gas with the sample at 600 °C. After reflection high energy electron diffraction showed a clear  $2 \times 1$  reconstructed surface,  $p$ -polarized SHG spectra were

acquired by tuning unamplified,  $p$ -polarized, 120 fs Ti:sapphire laser pulses, which were focused onto the sample at 55° incidence angle, from 710 to 800 nm. Fluence was kept low enough ( $<0.3 \text{ mJ/cm}^2$ ) that heating and carrier generation did not influence reflected SHG, which was normalized to a reference SHG signal [14]. B was then deposited by exposing the surface, at either room temperature (RT) or 600 °C, to diborane ( $\text{B}_2\text{H}_6$ ) gas. SHG spectra were acquired again. RT exposure leads to termination of Si dimer dangling bonds by  $\text{BH}_2$  and H [17]. At 600 °C, B tends to occupy second layer substitutional sites and to become electrically active, as shown by scanning tunneling spectroscopy [3,18]. Additional SHG spectra were acquired after exposing the latter surface (after cooling to 150 °C) to atomic H, generated by cracking back-filled  $\text{H}_2$  with a hot tungsten filament. Measurements were repeated with increasing dosages of  $\text{B}_2\text{H}_6$ . B coverage  $\theta_B$  for 600 °C deposition was calibrated with  $\sim 10\%$  accuracy by terminating this surface with atomic H at 150 °C, then comparing  $\text{H}_2$  temperature programmed desorption (TPD) with TPD of a standard H-B/Si surface for which  $\theta_B$  had been independently calibrated by Auger spectroscopy in a connected surface analysis chamber. For comparison, several 0.3  $\mu\text{m}$  thick epilayers with uniform *bulk* B doping of several  $10^{18} \text{ cm}^{-3}$  were also grown from diborane/disilane gas mixtures. SHG spectra were acquired for the clean and H-terminated bulk-doped films.

Figure 1a shows SHG spectra of clean Si(001) before (plus signs) and after (other data sets, except triangles) surface B adsorption at 600 °C for  $\theta_B$  up to  $\sim 0.3 \text{ ML}$ . The clean Si spectrum shows the surface  $E_1$  peak, redshifted (3.34 eV) from its bulk energy (3.4 eV) [19]. H termination quenches this feature (Fig. 1b, plus signs) as reported previously [14,19]. As  $\theta_B$  increases to 0.3 ML, the SHG signal from the H-free surface intensifies, and the  $E_1$  peak redshifts continuously to  $\sim 3.3 \text{ eV}$  (Fig. 1a). The SHG signal rises with time constant  $\sim 50 \text{ s}$  following

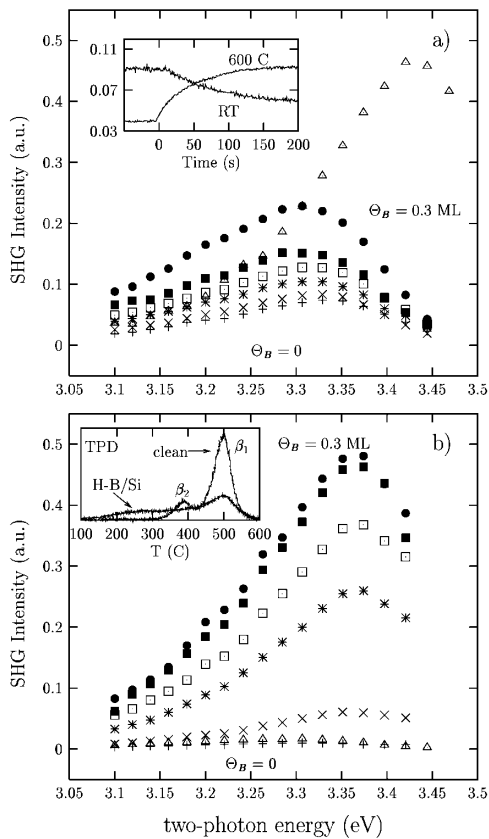


FIG. 1. SH spectra of (a) surface B-doped Si(001) and (b) H-terminated B/Si(001) surface.  $B_2H_6$  exposures are 0 L (plus signs), 2.4 L (crosses), 7.2 L (stars), 12 L (open squares), 24 L (filled squares), and 48 L (filled circles). Maximum  $\theta_B \sim 0.3$  ML. Triangles in (a) and (b) show SH spectra for bare and H-terminated bulk B doped samples, respectively. Inset of (a): real time SHG following  $B_2H_6$  exposure at 600 °C and RT, with  $B_2H_6$  partial pressure  $2 \times 10^{-7}$  Torr. Inset of (b):  $H_2$  TPD of H-Si(001) and H-B/Si(001).

opening of the  $B_2H_6$  inlet valve (see 600 °C curve in inset of Fig. 1a), a delay which we attribute to the time for second layer substitutional B to reach saturation coverage. For very low  $\theta_B < 0.02$  ML, H termination still quenches the SHG signal as for clean Si(001) (Fig. 1a and 1b, crosses). Surprisingly for higher  $\theta_B$ , H termination *intensifies* and *blueshifts* the spectral peak closer to the bulk  $E_1$  energy (Fig. 1b, upper four data sets), exactly opposite to the effect of H termination on clean Si(001).  $H_2$  TPD spectra for  $\theta_B = 0$  and 0.3 ML (inset of Fig. 1b) revealed, in addition to the dihydride  $\beta_2$  (380 °C) and monohydride  $\beta_1$  (500 °C) features, a broad low temperature (150 to 400 °C) desorption feature, which does not exist for undoped Si(001), and which has been identified with Si-H bonds weakened by charge transfer to underlying B backbonds [20]. With increasing  $\theta_B$  the latter peak intensifies at the expense of  $\beta_2$  and  $\beta_1$ . After selectively desorbing H associated with this low temperature feature by annealing the sample at 300 °C, most of the enhanced SH signal

shown in Fig. 1b was quenched. Thus H associated with this feature appears to be responsible for the surprising enhancement of SHG.

For contrast, the triangles in Fig. 1a and 1b show the SHG spectrum from the bare and H-terminated surface, respectively, of a *bulk* B-doped film. The former signal is 5 times stronger than from clean undoped Si and, in contrast to surface B-doped Si(001), the  $E_1$  peak is *blueshifted* to its bulk energy. This signifies the bulk origin of the signal via electric field induced second harmonic (EFISH) generation in the depletion region. H termination quenches and spectrally redshifts the SHG signal—again opposite to the behavior of surface B-doped Si(001)—because H passivates surface states responsible for Fermi level pinning [21], thus flattening the bands. A quantitative bulk EFISH analysis of such spectra is being published separately.

Surface  $B_2H_6$  adsorption at RT, in contrast to both 600 °C adsorption and bulk B doping, quenches surface SHG. This can be seen in the real time RT response at  $2\hbar\omega = 3.3$  eV shown in the inset of Fig. 1a. The  $\sim 100$  s rise time reflects primarily the surface accumulation time of  $B_2H_6$ , which subsequently dissociates into  $BH_2$  and H at Si dimer sites. Clearly the SHG response to second layer substitutional B differs markedly from that of either bulk B or nonsubstitutional surface  $B_2H_6$  dissociation products.

In order to understand this unique SHG response, we calculated SHG spectra using the *ab initio* pseudopotential (PP) method described in [15]. Pseudopotentials for Si and H were generated by the Bachelet-Hamann-Schlüter scheme [22] using the generalized gradient approximation (GGA). For B we used a soft-core pseudopotential generated by the Troullier-Martins scheme [23]. Because of the quantum-size shift our GGA  $E_1$  feature in the Si slab occurs near 3.4 eV. Therefore no quasiparticle corrections are needed for PP generated band structure. The surface structure was modeled as a slab of eight atomic (100) layers. Total energy minimization, using an energy cutoff of  $E_{cut} = 17$  Ry, yielded equilibrium atomic positions, according to the molecular dynamics method. For optical calculations we used up to  $E_{cut} = 31$  Ry. Although clean Si is well represented by a  $2 \times 1$  unit cell [15], the B-doped surface reconstructs in multidomain  $c(4 \times 4)$  [6] units. Computing the nonlinear optical properties of such a big unit cell is at present prohibitively lengthy for *ab initio* methods. Thus as a compromise, we limited the structural calculation to a  $2 \times 1$  unit cell also for B-doped surfaces, substituting B for one second layer Si and two H per surface Si-Si dimer (monohydride) for H-B/Si. *Ab initio* calculations for other Si-adsorbate systems showed that main SHG features were reproduced with this model as long as eigenfunctions were well converged [15]. In addition, using less computationally intensive semiempirical tight binding (SETB) methods discussed below, we have checked directly that larger unit cells yield similar qualitative behavior [24].

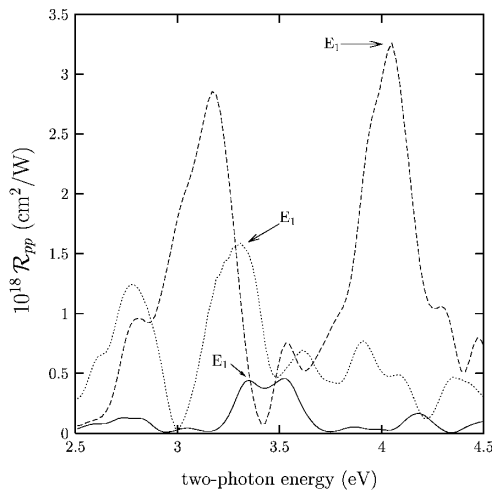


FIG. 2. *Ab initio* calculations of reflected SHG intensity  $\mathcal{R}_{pp}$  for clean (solid line), B-doped (dotted line), and H-B-doped (dashed line) Si(001)-(2  $\times$  1). Arrows identify the  $E_1$ -like feature in each curve.

Figure 2 shows calculated SHG intensity for clean B/Si and H-B/Si surfaces. For clean Si(001)-(2  $\times$  1), the  $E_1$  feature near 3.4 eV is evident. For B/Si a stronger, redshifted peak at 3.3 eV appears, in agreement with experiment, together with a second strong peak at 2.8 eV, beyond the experimental range. On H-B/Si, the former peak blueshifts to 4.05 eV, the latter to 3.1, and both strengthen. The qualitative behavior of the higher energy peak clearly mirrors the observed trends shown in Fig. 1. Quantitatively, the blueshift at H-B/Si is much stronger than observed. We believe the primary reason for this discrepancy is our use of a 2  $\times$  1 cell with one B, which overestimates maximum  $\theta_B$  by about a factor of 2. In fact, the surface monolayers from which SHG originates become alloyed at our modeled B and H concentrations, so that calculated peaks in Fig. 2 (in particular, on H-B/Si) lose identity as Si  $E_1$  and  $E_2$ . This situation can be remedied only with calculations based on larger unit cells. We also find that the blueshift at H-B/Si is sensitive to H concentration and bonding site. For example, using only 1 H per dimer, above either a Si or B backbond, we calculate that the same peaks are less blueshifted and broader. A mixture of such sites may be present experimentally.

The results presented in Fig. 2 describe the modifications of the SHG response in terms of chemical hybridization of surface bonds. These calculations make no explicit reference to the surface dc electric field  $\vec{E}_{dc}(z)$  approaching  $10^7$  V/cm, which accompanies electron transfer from surface Si dimers to second layer B acceptors [3,18]. Fields of this strength contribute to SHG in ways which are not completely included in the present PP calculations, since they significantly redistribute transition momentum (cf. Franz-Keldysh effect in linear optics) and induce higher-order SH polarization. A complete

accounting of these effects requires calculation of surface EFISH terms including both the *second*- and the *third*-order optical susceptibilities which is beyond current work. Nevertheless the results shown in Fig. 2 capture the main qualitative SHG trends observed for B/Si and H-B/Si.

To evaluate surface EFISH contributions more explicitly, we performed an independent SETB calculation of the electro-optical effects in SHG. Within the electric dipole approximation,  $\vec{E}_{dc}^s(z)$  was included phenomenologically into the TB Hamiltonian as a perturbation of potential energy along  $z$ . Relevant matrix elements were determined through matrix elements of  $z_{ij}$  (using unperturbed wave functions) [24], and evaluated by empirical fits to experimental linear optical functions [16]. Since TB parameters for the Si-B bond are not well established, we treated B as a Si atom for SETB calculations, while preserving atomic coordinates from the *ab initio* structure calculation.

The SETB SHG spectrum for clean Si(001)-(2  $\times$  1) clearly shows the  $E_1$  peak (Fig. 3, solid curve). The calculated  $E_1$  for B/Si (Fig. 3, dotted curve), with  $\vec{E}_{dc}^s$  directed inward with step-function magnitude  $0.9 \times 10^7$  V/cm terminating at the second layer B (Fig. 3, upper left inset), is intensified and redshifted compared to the undoped surface, in qualitative agreement with the measured spectra of Fig. 1a. Similar  $\vec{E}_{dc}^s(z)$  profiles yielded the same qualitative behavior; reversing the field direction reversed the direction of the spectral shift and substantially altered the intensity and line shape of the  $E_1$  peak.

H termination of B-backbonded Si dimers, according to our *ab initio* structure calculation, symmetrizes the surface dimer and quenches charge transfer to the second layer B, which should in turn quench the surface EFISH

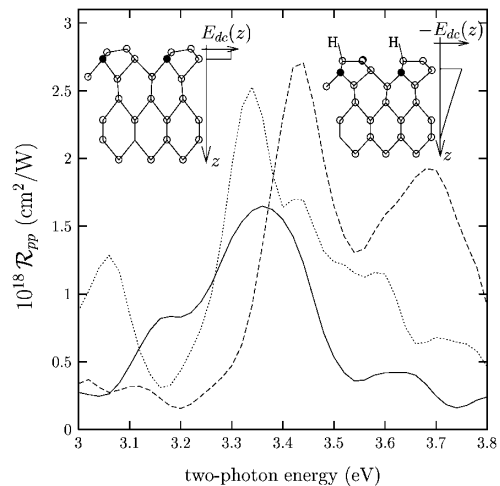


FIG. 3. SETB calculations of  $\mathcal{R}_{pp}$  for clean (solid line), B-doped (dotted line), and H-B-doped (dashed line) Si(100)-(2  $\times$  1). Energy is shifted upward by 0.48 eV. Insets: equilibrium structures viewed along [110]. Open (solid) circles are Si (B) atoms. Surface field  $E_{dc}(z)$  points toward bulk and vacuum, respectively, for B/Si (left) and H-B/Si (right).

polarization described above. Nevertheless, B can continue to act as a strong acceptor of electrons from the underlying bulk. Accompanied by redistribution of the space charge, this could create an electric field opposite in direction to, and deeper in spatial extent than,  $\vec{E}_{dc}^s(z)$ , as depicted in the upper right inset of Fig. 3. Its strength and spatial extent depend on band bending as determined by the relative energies of the acceptor states, which pin the surface Fermi level, and the bulk Fermi level. To illustrate the sensitivity of the SHG to the field profile changes we can anticipate field strength comparable to  $\vec{E}_{dc}^s(z)$  just beneath the second layer B and an accompanying EFISH contribution. Our SETB SHG spectrum for H-B/Si(001) (Fig. 3, dashed curve), using  $\vec{E}_{dc}^s(z)$  which starts abruptly at  $0.9 \times 10^7$  V/cm from the third layer, and decays exponentially with  $z$  (Fig. 3, upper right inset), shows the  $E_1$  peak near the bulk  $E_1$  energy and strengthened, in qualitative agreement with the experimental spectra of Fig. 1b. The  $E_1$  energy reflects the more bulklike origin of the signal and a field induced blueshift from the surface-directed  $\vec{E}_{dc}^s(z)$ .

In summary, SHG spectroscopy yields direct signatures of charge transfer accompanying second layer B incorporation at Si(001) which have been microscopically modeled. SETB confirms the key role of near-surface electric fields, which could not be neglected as compared to the effect of the rehybridization of atomic bonds. Our results shed light in the direction for further improvement of the theory by calculating the  $\vec{E}_{dc}^s(z)$  from the actual charge density, then incorporating its effect through a surface EFISH  $\chi_{ijkl}^{(3)}$  [24]. Experiments over a wider spectral range, and calculations based on more accurate structural units, will also improve quantitative interpretation of the spectroscopy.

This work was supported by the NSF Science and Technology Center Program (Grant No. CHE-8920120), the Robert Welch Foundation (Grant No. F-1038), Texas Advanced Research Program (Grant No. 0310-1999), and the Air Force Office of Scientific Research (Contract No. F49620-95-1-0475). B. S. M. acknowledges partial support from CONACyT (26651-E), Academia Mexicana de Ciencias, and Fundación México-Estados

Unidos para la Ciencia. V.I.G. and R.Q.W. acknowledge support of the U.S. Department of Energy (Grant No. DE-FG03-99ER14948).

---

\*Author to whom correspondence should be addressed.

Email address: downer@physics.utexas.edu

- [1] R. L. Headrick *et al.*, Phys. Rev. Lett. **63**, 1253 (1989).
- [2] H. Huang *et al.*, Phys. Rev. B **41**, 3276 (1990); R. L. Headrick *et al.*, Appl. Phys. Lett. **57**, 2779 (1990).
- [3] Y. Wang, R. J. Hamers, and E. Kaxiras, Phys. Rev. Lett. **74**, 403 (1995).
- [4] A. V. Zotov *et al.*, Phys. Rev. B **53**, 12 902 (1996).
- [5] P. Baumgärtel *et al.*, Phys. Rev. B **59**, 13 014 (1999).
- [6] J. Fritsch *et al.*, Phys. Rev. B **57**, 9745 (1998).
- [7] S. Wang, M. W. Radny, and P. V. Smith, Surf. Sci. **39**, 235 (1997).
- [8] P. J. Chen, M. L. Colaianni, and J. T. Yates, J. Appl. Phys. **70**, 2954 (1991); H. Kim *et al.*, J. Appl. Phys. **82**, 2288 (1997).
- [9] Y. Ma *et al.*, Phys. Rev. B **45**, 5961 (1992); T. M. Grehk *et al.*, Phys. Rev. B **52**, 11 165 (1995).
- [10] B. Gong *et al.*, Phys. Rev. B **59**, 15 225 (1999).
- [11] B. E. Weir *et al.*, Appl. Surf. Sci. **84**, 413 (1995).
- [12] Y. R. Shen, Nature (London) **337**, 519 (1989).
- [13] U. Höfer, Appl. Phys. A **63**, 533 (1996); P. Parkinson *et al.*, Appl. Phys. B **68**, 641 (1999).
- [14] J. Dadap *et al.*, Phys. Rev. B **56**, 13 367 (1997).
- [15] V. I. Gavrilenko *et al.* (to be published).
- [16] B. S. Mendoza, A. Gaggiotti, and R. Del Sole, Phys. Rev. Lett. **81**, 3781 (1998).
- [17] Y. Wang, J. Shan, and R. J. Hamers, J. Vac. Sci. Technol. B **14**, 1038 (1996).
- [18] Y. Wang and R. J. Hamers, Appl. Phys. Lett. **66**, 2057 (1995).
- [19] W. Daum *et al.*, Phys. Rev. Lett. **71**, 1234 (1993).
- [20] U. Höfer, L. Li, and T. F. Heinz, Phys. Rev. B **45**, 9485 (1992); H. Kim *et al.*, Appl. Phys. Lett. **69**, 3869 (1996).
- [21] Z. Xu *et al.*, J. Vac. Sci. Technol. B **15**, 1059 (1997).
- [22] G. B. Bachelet, D. R. Hamann, and M. Schlüter, Phys. Rev. B **26**, 4199 (1982).
- [23] N. Troullier and J. L. Martins, Phys. Rev. B **43**, 1993 (1991).
- [24] N. Arzate *et al.*, Appl. Phys. B **68**, 629–632 (1999).